A sponge transgenic mouse model reveals important roles for the miRNA-183/96/182 cluster in post-mitotic photoreceptors of the retina

Qubo Zhu[1], Wenyu Sun[2], Kiichiro Okano[1], Yu Chen[1], Ning Zhang[1], Tadao Maeda[1,3],

and Krzysztof Palczewski[1]

[1]Department of Pharmacology, School of Medicine, Case Western Reserve University, Cleveland, Ohio 44106-4965, USA; [2]Polgenix Inc., Cleveland, Ohio 44106, USA; [3]Department of Ophthalmology and Visual Sciences, Case Western Reserve University, Cleveland, USA.

Running Title: The miR-183/96/182 cluster in vertebrate retina.

[#]Address correspondence to: Krzysztof Palczewski, Ph.D., Department of Pharmacology, School of Medicine, Case Western Reserve University, 10900 Euclid Ave, Cleveland, Ohio 44106-4965, USA; Phone: 216-368-4631; Fax: 216-368-1300; E-mail: kxp65@case.edu

MicroRNA-183 (miR-183), miR-96 and miR-182 comprising the miR-183/96/182 cluster are highly expressed in photoreceptor cells. Although *in vitro* data have indicated an important role for this cluster in retina, details of its *in vivo* biological activity are still unknown. To observe the impact of the miR-183/96/182 cluster on retinal maintenance and light-adaptation, we generated a sponge transgenic mouse model that disrupted the activities of the three component microRNAs simultaneously and selectively in the retina. Although our morphological and functional studies showed no differences between transgenic and wild type mice under normal laboratory lighting conditions, sponge transgenic mice displayed severe retinal degeneration after 30 min exposure to 10,000 lux light. Histological studies showed that the outer nuclear layer thickness was dramatically reduced in the superior retina of transgenic mice. Real time PCR experiments in both the sponge transgenic mouse model and different microRNA stable cell lines identified Arrdc3, Neurod4, and caspase-2 (Casp2) as probable downstream targets of this cluster, a result also supported by luciferase assay and immunoblotting analyses. Further studies indicated that expression of both the cluster and Casp2 increased in response to light exposure. Importantly, Casp2 expression was enhanced in transgenic mice and inhibition of Casp2 partially rescued their light-induced retinal degeneration. By connecting the microRNA and apoptotic pathways, these findings imply an important role for the miR-183/96/182 cluster in acute light-induced retinal degeneration of mice. This study demonstrates a clear involvement of miRs in the physiology of post-mitotic cells *in vivo*.

MicroRNAs (miRs)[1] are endogenous short (about 22 nucleotides), non-coding RNA

---

[1] **Abbreviations used**: 3'-UTR, three prime untranslated region; Casp, caspase; GCL, ganglion cell layer; EGFP, enhanced-green fluorescent protein; ELM, external limiting membrane; ERG, electroretinography; ICC, immunocytochemistry; INL, inner nuclear layer; IPL, inner plexiform layer; IS, inner segment(s); OCT, optical coherence tomography; ONL, outer nuclear layer; OPL, outer plexiform layer; OS, outer segment(s); miR, microRNA; RPE, retinal pigmented epithelium; *wt*, wild-type.

1

molecules that bind to complementary sequences in the 3'-UTR of multiple target mRNAs, usually inhibiting their translation or causing their destabilization (1,2). MiRs are well conserved in eukaryotic organisms and widely expressed in different tissues and cell types (3). To date, 885 and 689 miRs have been identified in human and mouse genomes respectively (miRBASE Release 13.0, March 2009). Each miR regulates about 200-800 target genes, and sixty percent of protein-encoding genes in humans are predicted to be regulated by miRs (4). Several miRs are tissue specific, suggesting specialized roles in tissue differentiation and maintenance (5,6). Progress toward identifying the *in vivo* functions of miRs has been limited, not only by the complex biology of these molecules, but also by the experimental accessibility of the biological systems that they affect.

The retina is a layered tissue in the back of the eye that contains specialized photoreceptor cells called rods and cones as well as other cell types including ganglion, bipolar, horizontal, and amacrine cells (7). Its development, maintenance and light sensitive visual functions are highly regulated. At least 78 miRs are preferentially expressed in vertebrate retina (6,8,9), indicating the importance of miRs in modulating gene expression profiles in retinal cells. Moreover inactivation of Dicer (an essential RNase III endonuclease required for miR maturation) leads to progressive functional and structural degeneration of mouse retina (10,11).

In 2007, Xu *et. al.* identified miR-183, miR-96 and miR-182 as a sensory organ-specific paralogous miR cluster called the miR-183/96/182 cluster (6). These miRs are located within 4 kb of each other on mouse chromosome 6qA3 and transcribed in the same direction from telomere to centromere. This genomic arrangement is highly conserved in vertebrates (Fig. S1A), and the sequences of the three component miRs are similar to each other. Real time PCR and in *situ* hybridization data reveal that the miR-183/96/182 cluster is highly expressed in photoreceptors and interneurons of the inner nuclear layer but is not detectable in brain (6,12). Levels of the cluster are down-regulated during dark-adaptation and up-regulated in light-adapted retina, with rapid decay and increased transcription being responsible for the respective changes (13). In the Pro347Ser rhodopsin transgenic mouse, a human retinitis pigmentosa model, and three other photoreceptor-linked mouse models of RP (*Opsin$^{-/-}$, Δ307* and rds) (12), expression of the miR-183/96/182 cluster was dramatically decreased (12), suggesting that such decreased expression is associated with retinal disease. However, another study showed that there were no significant transcriptional or phenotypic changes in miR-182 depleted mice (14). Similarly, a naturally occurring seed region substitution mutation in miR-96 of human patients did not produce any detectable visual impairment (15). The absence of retinal defects in these cases may stem from redundancy in the miR-183/96/182 cluster, *i.e.,* because the three component miRs are similar, they can functionally substitute for each other.

Exposure to excessive white light can induce retinal degeneration in a variety of animals. However, the molecular mechanism by which light induces retinal degeneration is presently unclear. Apoptosis has been implicated as a common final pathway in retinal degeneration (16), and several apoptosis-related genes have been shown to be activated during photoreceptor cell death. Casp1 and Casp2 were detected in the ONL of degenerating rat retina (17). BID and its upstream gene, *p38*, were also activated in apoptotic photoreceptors (18). Bax and Bak double knockout in mice protected photoreceptors from light damage (19,20). Moreover, inhibition of Casp3 preserved the retina in *rd1/rd1* mice (21), tubby mice (22) and S334ter rats (23). Casp2 is a cysteine-aspartate protease that mediates apoptosis induced by many types of cellular stress, including reactive oxygen species (ROS), DNA damage, and endoplasmic reticulum (ER) stress. Once activated, Casp2 cleaves BID and causes mitochondrial outer membrane permeabilization (MOMP) and cytochrome C release, which in turn activates Casp9 and Casp3, resulting in apoptosis (24).

To clarify the roles of the miR-183/96/182 cluster in retinal maintenance and light-adaptation, we generated a sponge transgenic mouse model to disrupt the activity of these three miRs simultaneously in the retina. Then we characterized the retinal defects in these transgenic mice and identified transcriptional changes in their retinas. Although there were no significant morphological and functional differences between wild type (*wt;* C57/BL6) and transgenic mice under laboratory cyclic lighting conditions, transgenic mice displayed severe retinal degeneration after acute bright light exposure.

Materials and Methods

Generation of the sponge transgenic mouse model – To generate miR-183/96/182 cluster sponge elements, we introduced 10 copies each of complementary sequences to miR-183, miR-96 and miR-182, each with mismatches at positions 9–12 for improved stability (25), into the 3′-UTR of enhanced green fluorescent protein (EGFP) in a pNOVA expression vector. Sponge element expression was driven by a opsin promoter and terminated with an SV40 polyadenylation element (Fig. S2A). Special primer pairs bridging the opsin promoter and EGFP coding sequences were designed for PCR detection. To assess the specificity and efficiency of the opsin promoter, the plasmid was sequenced and then transfected into Y79 cells (retinal carcinoma cells, American Type Culture Collection, Manassas, VA) and HEK293 cells (controls). Bright EGFP positive cells were noted in the transfected Y79 cells, but not in the non-transfected cells or HEK293 cells, confirming the efficiency and specificity of the opsin promoter (Fig. S2B). The 6.8 kb transgene fragment was cut out by NotI and MluI, and then injected into fertilized eggs of BL6/SJL hybrid mice using the pronuclear injection method in the Transgenic and Targeting Facility at Case Western Reserve University. Founder mice were then back crossed with C57/BL6 mice many times to obtain a clean background.

Genotyping analyses – Genomic DNA from the tails of 4-week-old mice was digested with DirectPCR (VIAGEN Biotech Inc., Los Angeles, CA) plus proteinase K (final concentration: 50 µg/ml) at 55 °C overnight and then heat-inactivated at 85 °C for 45 min. Sequences of primer pairs used to screen the sponge transgenic mice were: SpongeFor: 5′-ATATCTCGCGGATGCTGAAT-3′; SpongeRev: 5′-GAACTTCAGGGTCAGCTTGC-3′.
Rd_For/Pde_Rev and Pde_For/Pde_Rev primer pairs were designed to distinguish the *Pde6b^rd1* mutant allele from the normal allele. β-Actin, detected by β-actin_For/β-actin_Rev primer pairs, was used as an internal control. Sequences for these primers were: Rd_For, 5′-CCAGTGGCCTTCCAACCTAA-3′; Pde_For, 5′-CCAGTGGCCTTCCAACCTAC-3′; Pde_Rev, 5′-GAAAGTTGAACATTTCATCAGCTG-3′. β-actin_For: 5′-AGTGTGACGTTGACATCCGTA-3′; β-actin_Rev: 5′-GCCAGAGCAGTAATCTCCTTCT3′.

RT-PCR and Real time PCR – Total RNAs were extracted from the mouse retina or cells with the mirVanaTM miR Isolation Kit (Ambion, Austin, TX). For miR real time PCR, all reagents, including the Universal cDNA Synthesis Kit, SYBR® Green master mix, LNA™ PCR primer sets and 5S rRNA PCR primer set, were purchased from Exiqon (Woburn, MA). For mRNA RT-PCR and real-time PCR, primer sets were designed within exon junction areas listed in Table S1. In brief, mRNAs were reverse transcribed with a SuperScript® III First-Strand Synthesis kit (Invitrogen, Carlsbad, CA). Then 50 ng cDNA was mixed with FS Universal SYBR Green Master (Roche, Mannheim, Germany) and the target gene primer set (final concentration: 1 µM for each primer) to produce a 20 µl reaction mixture. All real time PCR experiments were done in an Eppendorf Mastercycler, ep realplex real time PCR system.

Splinted ligation – Total RNAs were extracted from mouse retina or cells with the mirVanaTM miR isolation kit and 0.5 - 4 µg of total RNA was used for each assay. All procedures followed manufacturer's instructions for the miRtect-IT miRNA Labeling and Detection Kit (USB, Cleveland, OH) (26). Twenty pmol of detection oligonucleotide was 5′-end radiolabeled with 2.5 µM [γ-^{32}P] ATP (150 mCi/mL, Perkin-Elmer,

Akron, OH). Designs of bridge oligonucleotides and mimic oligonucleotides were based on miR sequences registered in the miRBase Sequence Database (http://microrna.sanger.ac.uk/sequences/) (see Table S2). Ligated DNA-RNA complexes were separated by 16% mini urea-polyacrylamide gels and exposed to phosphor screen after drying for 2 h. The radio-isotope signal detected by the phosphor screen was recorded with Storm 820 (Amersham Biosciences, Chandler, AZ). Because the miR-183 miR-96 and miR-182 sequences are similar, we tested the probe specificities before doing the experiments (Fig. S3).

Electroretinography (ERG) – Two- to four-month-old female mice were dark-adapted for more than 24 h prior to an ERG and then anesthetized by intraperitoneal injection of a mixture (20 µL/g body weight) containing ketamine (6 mg/mL) and xylazine (0.44 mg/mL) in 10 mM sodium phosphate, pH 7.2, with 100 mM NaCl. To stabilize body temperature, mice were placed on a heated pad (<40 ^{o}C) in a Ganzfeld chamber and positioning of the contact lens electrodes was adjusted. Then two needle electrodes were placed under the skin of the forehead and tail. Before the start of recording, the base line was checked to verify that the mouse was alive and the lens was well contacted. Single flash ERGs were recorded simultaneously from both eyes, with scotopic flash ERGs from −3.7 to 0.6 log cd·s/m^2 (interstimulus intervals between 10 s and 60 s). After 5 min of light adaptation (30 cd/m^2), photopic flash ERGs from -2.1 to 0.6 log cd·s/m^2 were recorded. Amplitudes were measured by EM software for Windows (LKC Technologies, Inc) from baseline to the negative peak for a-waves, and from the latter (or baseline, if absent) to the positive peak for b-waves.

Ultra–high-resolution optical coherence tomography (OCT) – Ultra-high resolution SD-OCT (Bioptigen) was employed for *in vivo* imaging of mouse retinas. Mice were anesthetized by i.p. injection of a mixture (20 µL/g body weight) containing ketamine (6 mg/mL) and xylazine (0.44 mg/mL) in 10 mM sodium phosphate, pH 7.2, with 100 mM NaCl. Pupils were dilated with 1% tropicamide. Four pictures acquired in the B-scan mode were used to construct each final averaged SD-OCT image. The superior retina, inferior retina and optical nerve head regions were imaged for each eye.

Retinal histology and immunocytochemistry (ICC) – Mouse eyeballs were extracted immediately after euthanasia. After removal of the cornea and lens, eyecups were fixed in 4% neutral formalin overnight at 4 ^{o}C. Following 5%, 10% and 20% sucrose dehydration, eyecups were embedded in 20% sucrose/OCT (1:1), and 12 µm thick sections were cut. Hematoxylin and eosin (H&E) staining was performed by the Pathology core facility at Case Western Reserve University. For immunocytochemistry, slides were incubated for 2 h at 55 ^{o}C, then blocked with 1.5% normal goat serum (NGS) for 1 h, and incubated with primary antibody overnight. After washing 3 times in PBS (137 mM NaCl, 2.7 mM KCl, 4.3 mM Na2HPO4, 1.4 mM KH2PO4; pH 7.2 to 7.4), slides were incubated with fluorescent conjugated secondary antibody, peanut agglutinin lectin (PNA: for detection of cones, 1: 500 dilution) and DAPI (for counterstaining cell nuclei, 1: 500 dilution). The primary antibody was anti-opsin 1D4 antibody (1: 200 dilution, a kind gift from R. S. Molday (Vancouver, BC, Canada)).

Laser Capture Microscope (LCM) - LCM was done in the core facility in Cleveland Clinic Foundation. Basically, 24 h after 30 min 10,000 lux light exposure, eye balls from 4-month-old mice were collected and fresh Tissue-Tech O.C.T. compound. All samples were cut at 12 µm thickness and mounted on Leica membrane slides (PET-Membrane, Wetzlar, Germany). Rapid HistoGene® Stain (Applied Biosystems, Foster City, CA) staining was used to identify different regions of the retina. Briefly, the sections were fixed in 75% ethanol for 30 s, and then immersed in HistoGene Staining Solution for 30 s, followed by dehydration and wash with graded alcohols (75%, 95%, and 100%) for 20 s each. Regions of the retina were isolated using an HC PLan Fluotar 10X/0.3NA lens on a Leica AS-LMD Laser Microdissection microscope (Leica Microsystems, Bannockburn, IL) equipped

4

with a 337nm nitrogen laser and a Hitachi HV-C20A 3-chip color CCD camera. Fragments were collected in lysis buffer of mirVana™ miR Isolation Kit for late experiment.

Creation of stable cell lines – Partial pri-miR sequences of miR-183, miR-96 and miR-182 were inserted into pMXs-IRES-EGFP retroviral vector (Fig. S4A), and the plasmids were transfected into Phoenix cells with calcium phosphate. Medium was replaced 12 h after transfection and the transfected cells were incubated for 24 h at 32 $^{\circ}$C. Viruses were harvested from the medium and diluted 1:6 with target cell medium, then supplied with polybrene (final concentration 5 µg/ml). NIH3T3 cells were incubated with this virus mixture at 32 °C supplemented with 5% CO_2. After 3 cycles of viral infection, NIH3T3 cells were treated with 0.05% trypsin (Thermo Scientific, Logan, Utah) for 2 min to dissociate them from the plates. Then cells were sorted to obtain those 5% with the greatest EGFP fluorescence intensity as assessed by flow cytometry at the Flow Cytometry Core Facility at Case Western Reserve University.

Immunoblotting – Cells or retinas were lysed in NTEN buffer (100 mM NaCl, 0.5% NP-40, 50 mM Tris–HCl, pH 7.6) with a proteinase inhibitor cocktail (Roche). Proteins were separated by 15% polyacrylamide gels and detected by anti-Casp2 (1: 200 dilution, Biovision, Mountain view, CA), anti-opsin 1D4 (1: 1,000 dilution), anti-BID (final concentration 1 µg/mL, R&D Systems, Minneapolis, MN), anti-middle-wave-sensitive opsin (mv-opsin, 1: 500 dilution, EMD Millipore, Billerica, MA) and anti-β-tubulin (1: 1,000 dilution, Santa Cruz, Santa Cruz, CA) antibodies.

Luciferase reporter assay – pGL3P-4XNeurod4-3'-UTR, pGL3P-4XArrdc3-3'-UTR and pGL3P-4XCasp2-3'-UTR plasmids were constructed for the luciferase reporter assay. Basically, four copies of targeted regions from the target gene 3'-UTR flanked by Xb1II and FseI restriction sites were inserted between the Luc coding sequence and SV40 polyadenylation element of the pGL3-promoter vector (pGL3P) (Fig. S5A). NIH3T3 cells were maintained in DMEM medium with 10% FBS and transfections were carried out with the Lipofectamine™ 2000 reagent (Invitrogen). After obtaining the engineered plasmids, we first tested their linear expression range (Fig. S5B). Plasmids overexpressing miR-183/96/182 clusters were constructed by inserting partial pri-miR sequences of miR-183, miR-96 and miR-182 into the pRNAT-CMV3.1 vector (Fig. S2A). For miR targeting assays, cells were cultured in 24-well plates and transfected with 500 ng of control pRNAT-CMV3.1 vector or plasmids overexpressing miRs-183, -96, or -182 along with 160 ng of a reporter construct, either pGL3P-4XNeurod4-3'-UTR, pGL3P-4XArrdc3-3'-UTR, pGL3P-4XCasp2-3'-UTR or empty pGL3P. Forty ng of pRL-CMV-Renilla plasmid was also transfected as an internal control. Expression levels of miR-183, miR-96 and miR-182 were measured by EGFP fluorescence. The luciferase reporter assays (Promega, Madison, WI) were performed 48 h after transfection, and luciferase activity was determined with an Lmax™ Microplate Luminometer (Molecular Devices, Sunnyvale, CA). Relative luciferase activities were calculated as ratios of firefly to rellina luciferase activities.

Light induced retinal damage – Two- to four-month-old mice were dark adapted for 1 week before use for light induced retinal damage experiments. After pupillary dilation by 1% tropicamide, mice were exposed to white fluorescent light (10,000 lux) (150-watt spiral lamp, Commercial Electric, Cleveland, OH) for either 10 or 30 min in a white bucket (Papersmith, San Marcos, TX) and then kept under normal cyclic light conditions. No more than 2 mice were kept in a bucket at the same time. OCT examination was performed 2 weeks after light exposure.

Effect of caspase 2 inhibitor on light induced retinal damage – Two- to four-month-old mice were dark adapted for 1 week before use for the caspase 2 inhibitor experiment. After pupillary dilation with 1% tropicamide and exposure to 10,000 lux white light for 30 min, mice were anesthetized by i.p. injection of a mixture (20 µL/g body weight) containing ketamine (6 mg/mL) and xylazine (0.44 mg/mL) in 10 mM sodium phosphate, pH 7.2, with 100 mM NaCl. One µl of Z-VDVAD-FMK (R&D

5

Systems, Minneapolis, MN; 1.6 mM in 2% DMSO) was injected intravitreally into the right eyes with a NanoFil 100 μl syringe (World Precision Instruments, Sarasota, FL) and a 33 gauge needle (World Precision Instruments). Left eyes were injected in parallel with 2% DMSO as the control. After injection, a drop of antiseptic solution (Daiichi Sankyo Company Limited, Tokyo, Japan) was applied to the cornea. OCT examination and immunocytochemistry analysis were performed 2 weeks later.

Statistical analyses – Results are presented as mean ± standard deviation (SD) and the number of experiments is indicated. ImageJ 1.42q (National Institutes of Health, USA) was used for quantification. Statistical significance was assessed by using the two-tailed Student's *t*-test.

Results

The miR-183/96/182 cluster is specifically expressed in photoreceptor cells – To determine whether miR-183/96/182 cluster miRs are expressed in rods and/or cones, we used two knockout mouse models of photoreceptor degeneration. Cones are absent in *Cone-DTA*^{+/-} mice but the density and morphology of rods are normal (27). In contrast, neither cones nor rods are present in 4-month-old *Opsin*^{-/-} mice (28). Total RNAs from the retina of 4-month-old *wt*, *Cone-DTA*^{+/-} and *Opsin*^{-/-} mice were extracted and subjected to splinted ligation to measure miR abundance with the ubiquitous miR, let-7, used as an internal control. None of the three miRs showed any changes in *Cone-DTA*^{+/-} mice, but all were significantly reduced in *Opsin*^{-/-} mice (Fig. 1A). MiR-107, known to be expressed in human and rat retina (8), exhibited little change in the splinted ligation assay. The reduced expression of miRs -96, -182, and -183 in *Opsin*^{-/-} mice strongly suggests that these miRs are expressed in photoreceptors. But as cones account for fewer than 5% of total photoreceptors, it is unclear whether these miRs are expressed in cones as well.

To confirm expression of the miR-83/96/182 cluster in photoreceptor cells we examined its expression in RNA isolated from the retina of 4-month-old mutant mice with either retinal degeneration (*rd1/rd1* mice) or the P23H opsin mutation, both of which lack photoreceptors but retain the remaining cellular constituents of neural retina (29,30). Splinted ligation results showed that, compared to wild-type (*wt*) retina, miRs-183, -96 and -182 were decreased 2.4-, 2.0- and 2.1-fold, respectively in *rd1/rd1* mutant retina, and 2.3-, 2.0- and 2.5-fold, respectively, in P23H opsin mutant retina (Fig. 1B). miR-125a (which is expressed in retina, brain, and other organs (12)) and the ubiquitous miR let-7 were used as controls for this assay. Expression of let-7 was unchanged in both *rd1/rd1* mutant and P23H opsin mutant retinas, and miR-125a showed a modest increase in expression (1.4- and 1.6-fold in *rd1/rd1* and P23H opsin mutant retina). Thus, miR-183, miR-96 and miR-182 were all specifically decreased in retinas of mutant mice that exhibited different types of photoreceptor degeneration, suggesting that miR-183/96/182 clusters are highly expressed in photoreceptor cells.

Creation of miR-183/96/182 cluster sponge transgenic mice – miR-183/96/182 miRs share significant sequence similarity in their seed regions (Fig. S2Ab). Indeed, there is extensive overlap in the predicted targets of these three miRs. This functional redundancy complicates interpreting the results of disrupting each member of this cluster. To overcome this problem and better understand the roles of the miR-183/96/182 cluster *in vivo*, we generated miR-183/96/182 cluster sponge transgenic mouse lines. The miR-183/96/182 cluster sponge element was composed of 10 copies each of sequences complementary to miR-183, miR-96 and miR-182 with mismatches at positions 9–12 to enhance stability. This sequence was inserted into the 3′-UTR of EGFP in a pNOVA expression vector regulated by a opsin promoter and ending with a SV40 polyadenylation signal (Fig. S2A). Several transgenic mouse lines were confirmed by PCR analyses of genomic DNAs. Because the target sequence was injected into fertilized eggs of BL6/SJL hybrid mice and there is a retinal degeneration allele *Pde6b*[rd1] harbored in SJL background mice, we also eliminated *Pde6b*[rd1] mutant mice after genotyping PCR analyses. Three transgenic mouse lines were established and analyzed (Fig. 2Aa). Real time PCR analyses of F1 genomic DNA showed that line

6

SP#1231 harbored the highest copy number of the transgene, followed by SP#1135 and SP#1128. The transgene numbers were 7.0±1.0, 2.1±0.4 and 1.3±0.1 copies per haploid genome, respectively (calculated by real time PCR, Fig. S6A and Fig. 2Ab).

Though miR sponge elements are designed to disrupt miR activity by sequestering mature miRs, introduction of a miR sponge can alter miR levels in some cases (31). To determine whether sponge components were transcribed, and the endogenous miR-183/96/182 cluster levels changed, total RNAs from retinas of transgenic and *wt* mice were extracted and analyzed by semi-quantitative RT-PCR or splinted ligation. Semi-quantitative RT-PCR demonstrated that line SP#1231 expressed the highest level of the sponge element in the retina, followed by lines SP#1135 and SP#1128 (Fig. 2Ba). The splinted ligation assay showed only a marginal decrease of miR-183, miR-96 and miR-182 in all three sponge transgenic mouse lines (Fig. 2Bb, Fig. S6B). This result, consistent with that of a previous study (13), indicates that our sponge element disrupted the activity of the miRs primarily by sequestration rather than destabilization. To verify the spatial expression pattern of sponge elements, we measured sponge element expression levels in different tissues of sponge transgenic mice by RT-PCR. This revealed that the sponge element mRNA was detectible only in retina and not in brain, heart, liver or intestine (Fig. S6C). We also tested whether endogenous opsin expression was affected by the presence of multiple opsin promoter elements in these transgenic mice. Immunoblotting results showed that opsin expression levels were similar in *wt* and all three transgenic mouse lines (Fig. S6D).

Bright light induces severe retinal degeneration in miR-183/96/182 cluster sponge transgenic mice – Because levels of the miR-183/96/182 cluster decreased dramatically in mutant mouse models of retinal degeneration (Fig. 1)(12), we tested whether inhibition of the miR-183/96/182 cluster in sponge transgenic mice would result in retinal degeneration. To our surprise, no morphologic or functional changes in retinas from either 2- or 6-month-old transgenic

mice were identified by histological or ERG analysis (data not shown).

Considering that the miR-183/96/182 cluster was previously shown to be up-regulated in response to light (13), we hypothesized that these miRs might play a role in protecting the retina from acute light-induced retinopathy. Both *wt* and sponge transgenic mice were exposed to 10,000 lux white light for 10 or 30 min. Then OCT and H&E staining of retinas were performed 2 weeks later. In the superior retina, sponge transgenic mice exhibited a 30% ± 3% loss of photoreceptors after 10 min light exposure and an 80% ± 5% loss after 30 min exposure, whereas *wt* control mice exhibited no significant retinal degeneration after either exposure (Fig. 3A and 3B). To distinguish retinal rods from cones, we performed immunocytochemistry with 1D4 antibody (rods) and PNA (cones). After the 10 min light exposure, rod cell death was noted and both the outer segment and outer nuclear layer were thinner, but cone damage was less pronounced. After 30 min exposure, rods had almost disappeared and few cones remained. With support from rods lacking, the remaining cones were highly disordered (Fig. 3Ca). This phenotype was confirmed by immunoblotting. In transgenic mouse retina, the opsin level decreased by 30% and 60% after 10 min and 30 min light exposure. But the mw-opsin level decreased only slightly after 30 min light exposure. Both opsin and mw-opsin levels remained unchanged in wild type mouse retina (Fig. 3Cb, Table S3). It should be noted that the EGFP expression did not cause retinal degeneration because EGFP expression in transgenic mice was not reliably detected by immunocytochemistry. Repetitive miR-183/96/182 complimentary sequences in the 3'-UTR of EGFP likely blocked the EGFP expression.

The vulnerability of transgenic mouse retina to intense light differed by region. Thus, ONL thickness in the inferior retina was nearly identical in unexposed and light-stressed mice, but in the superior retina it decreased from about 50 μm to 20 μm after light exposure in transgenic mice (Fig. 4A and 4B). To check whether the regional selectivity of light-induced retinal degeneration was related to the spatial expression pattern of miR-183/96/182 cluster, we

examined the expression level of miR-183, miR-96 and miR-182 in both inferior and superior retina under different conditions by laser-capture microscopy and LNA-based real time PCR. LNA-based real time PCR indicated no difference between the superior and inferior retina in the expression of these three miRs although miR-96 and miR-183 but not miR-182 increased after 30 min light exposure in both *wt* and transgenic mice (Fig. 4C). The number of transgene copies did not affect this result as this phenotype was reproducible in all three transgenic mouse lines (Fig. 4A). Thus sponge transgenic mice displayed severe degeneration of the superior retina after 30 min of intense light exposure.

Identification and validation of potential target genes of miR-183/96/182 cluster miRs – To better understand the biological roles of miR-183/96/182 cluster miRs in mouse retina, we compiled a list putative target genes of the miR-183/96/182 cluster by using three computational target prediction algorithms: PicTar (http://pictar.mdc-berlin.de/), TargetScan 5.1 (http://www.targetscan.org) and MicroCosm (http://www.ebi.ac.uk/). We also identified genes expressed in *wt* retina by massive parallel RNA sequencing (32). Of all putative targets, we focused only on those expressed in retina with 3'-UTRs conserved in vertebrates. Several targets with functions involved in nervous system development, photo-transduction, visual cycle, circadian rhythm or apoptosis are listed in Table 1. These targets were validated by real time PCR with GAPDH used as an internal control. Four genes out of 11 candidates, namely Arrdc3, Neurod4, Clock and Casp2 (Fig. 5A), showed significantly increased expression in transgenic mice. Arrdc3 is an arrestin domain-containing protein which can recruit the NEDD4 E3 ubiquitin ligase (33) important for nervous system development. Neurod4 is involved in the differentiation of horizontal, amacrine and bipolar cells (34); repression of its expression in photoreceptors could adversely affect photoreceptor cell fate. Clock, the core component of the circadian clock, forms a heterodimer with Bmal1 and binds to circadian E-box promoter elements that enhance the transcription of Period 1 and 2 and cryptochrome 1 and 2 (35). Casp2 mediates apoptosis induced by many cellular stresses, including reactive oxygen species, endoplasmic reticulum (ER) stress and DNA damage (24). We further confirmed these target genes by repeating the real time PCR experiment with all three transgenic mouse lines, using their littermates as controls. All four genes were up-regulated in these cell lines although some increases were not statistically significant (Fig. 5B).

Having demonstrated that disruption of the miR183/96/182 cluster leads to upregulation of these candidate target genes, we next wanted to confirm that these genes can be directly targeted by these miRs. Thus we established stable cell lines over-expressing miR-183, miR-96 and miR-182, respectively. Partial pri-miR sequences packed in pMXs-IRES-EGFP retrovirus (Fig. S4A) were used to infect NIH3T3 cells and the top 5% of cells exhibiting the greatest EGFP fluorescence intensity were sorted and saved as over-expressing stable cell lines. First, we confirmed miR expression levels in these three cell lines for both pri-miRs (Fig. S4Ba) and mature miRs (Fig. S4Bb) by RT-PCR and splinted ligation. Next, we measured the effect of miR over-expression on the expression of putative miR-183/96/182 target genes. mRNA levels of Arrdc3 were 38% lower in miR-96 stable cells than NIH3T3 cells, but showed little change in miR-182 stable cells and increased 1.3-fold in miR-183 stable cells. Clock's mRNA level remained the same in all cell lines. mRNA levels of Casp2 dropped to 42% and 57% in miR-96 and miR-182 stable cells, but exhibited no change in miR-183 stable cells (Fig. 5Ca). Neurod4 was barely detectable in NIH3T3 cells, so we could not evaluate its reaction to the miR-183/96/182 cluster in over-expressing cell lines. Immunoblotting analyses were also performed with extracts of all cell lines with β-tubulin used as an internal control. Casp2 antibody, which recognizes both the 49 kDa pro-Casp2 and 12 kDa cleaved-Casp2, revealed that both pro-Casp2 and cleaved-Casp2 were decreased in miR-96 and miR-182 stable cells but not in miR-183 stable cells (Fig. 5Cb, Table S4).

To further evaluate the role of the miR-183/96/182 cluster in regulating its target genes, we generated luciferase reporters with four copies of the predicted target regions from the 3'-UTR of each target gene, and co-transfected the

8

reporters with miR-183, miR-96 and miR-182 over-expression plasmids. These luciferase assay results showed that miR-96 repressed luciferase activity by 47% in the reporter derived from the Arrdc3 targeted region, 57% for Neurod4 and 57% for Casp2 as compared with the empty vector. miR-182 repressed luciferase activity by 41% for Arrdc3 and 39% for Casp2 compared with the empty vector; and miR-183 had no effect on any target genes. As a negative control, luciferase activity of cells containing the empty pGL3P vector was not affected by any miR-183/96/182 cluster miR. No obvious additive effects were detected when miR-96 and miR-182 or all three miRs were transfected together (Fig. 5D). These reporter assays provide clear evidence that miR-96 specifically targets the 3'-UTR of Arrdc3, Neurod4 and Casp2; miR-182 specifically targets the 3'-UTR of Arrdc3 and Casp2; and miR183 does not affect the 3'-UTR of any of the tested target genes. Taken together, the above data indicate that Arrdc3, Neurod4 and Casp2 are targets of miR-183/96/182 cluster miRs.

Repression of Casp2 expression is one reason that miR-183/96/182 cluster miRs protect the retina from light induced degeneration – Bright light-induced retinal degeneration is thought to be Casp-dependent (36,37). Because miR-183/96/182 sponge transgenic mice showed severe acute light-induced retinal degeneration and Casp2 was one of the targets of miR-183/96/182, we hypothesized that repression of Casp2 expression was one reason why the miR-183/96/182 cluster protected against light induced retinal degeneration. To test this hypothesis, we first measured Casp2 mRNA levels, as well as cluster miR levels in *wt* mice after a 30 min 10,000 lux white light exposure. Real-time PCR results revealed an increase of Casp2 after light exposure (Fig. 6Aa) similar to that reported in Sprague-Dawley rats (36). Casp2 mRNA peaked at 12 h after light induction, and the fold change was about 1.8±0.1. Splinted ligation results showed that miR-183 and miR-96 but not miR-182 increased significantly 12 to 24 h after light exposure (Fig. 6Ab, Table S5). These experiments were repeated twice and densitometric analysis indicated that miR-96 and miR-183 expression in animals 24 h after light

exposure were 2.5 and 2.1-times higher than in dark-adapted mice, whereas miR-182 expression remained unchanged.

Data in *wt* mice suggested that miR-183/96/182 cluster miRs and Casp2 are both regulated similarly after bright light exposure. So we measured Casp2 expression in sponge transgenic mice after light exposure. Both *wt* and transgenic mice were exposed or unexposed to light. Then retinas were collected and total RNA and protein were isolated to determine Casp2 levels. Both real-time PCR and immunoblotting results showed that without protection against degeneration by miR-183/96/182 cluster miRs, Casp2 levels increased much more in response to bright light in transgenic mice than in *wt* mice (Fig. 6Ba and 6Bb, Table S6). As predicted, cleavage of BID, a substrate of Casp2 (24), also was enhanced in transgenic mice after bright light exposure (Fig. 6Bb, Table S6).

To check whether inhibition of Casp2 could protect the retina against light-induced damage in transgenic mice, the Casp2 inhibitor Z-VDVAD-FMK was injected intravitreally into the right eyes of both *wt* and transgenic mice before light exposure; 2% DMSO in PBS was injected into the left eyes of the same mouse as a control. Immunocytochemistry results showed that, compared to the pseudo treatment in left eyes, Z-VDVAD-FMK partially relieved light-induced retinopathy in the right eyes of transgenic mice (Fig. 6C). In transgenic mice, the ONL thickness of Z-VDVAD-FMK-treated retina was about 30 μm in the superior area but only about 20 μm in the comparable area of DMSO-treated retina. In *wt* mouse retina unaffected by either the light exposure or the treatment, the ONL thickness was about 50 μm (Fig. 6D). Immunoblots also demonstrated that Z-VDVAD-FMK treatment can slightly attenuate the decrease of both rod opsin and mw-opsin after light exposure in transgenic mice. Statistical analyses showed that without Z-VDVAD-FMK treatment, the opsin level in transgenic mouse retina was only 40% that of *wt* retina after light exposure whereas the mw-opsin level was 70% that of *wt* retina. With Z-VDVAD-FMK treatment, however, the opsin level in transgenic mouse retina was 50% of that of *wt* retina and the mw-opsin level even marginally increased relative to that in *wt* retina after light exposure (Fig. 6E).

9

Discussion

This research reveals an important role for the miR-183/96/182 cluster in protecting against bright light-induced retinal degeneration *in vivo* and identifies a connection between this cluster and an apoptotic pathway. The findings highlight yet another protective mechanism against light-induced photoreceptor degeneration, and also demonstrate a clear role of miRs in a post-mitotic tissue *in vivo*. The observed phenotype is unambiguous, and manifest when miR-183/96/182 cluster miRs are simply sequestered rather than altered.

Exposure to excess light induces photoreceptor apoptosis, which has been used as a model for previous studies of retinal degeneration. However, the underlying pathogenic mechanisms remain obscure. Here we provide evidence for involvement of the miR-183/96/182 cluster in this process. Repression of Casp2 expression appears to be one mechanism by which this cluster protects mice against retinal degeneration after bright light exposure (Fig. 7).

Involvement of caspases in retinal light-induced damage is still under active investigation. Chahory *et al.* (38) did not observe Casp3 activation in the retina of Fisher rats after bright light exposure and a similar result was obtained in Balb/c mice by Donovan *et al.* (39). But other studies reported activation of both Casp3 and Casp2 after light exposure in Sprague-Dawley rats (36) and implicated caspase proteases in retinal degeneration by showing that inhibition of Casp1 or Casp3 reduced photoreceptor cell death (37). Differences in light intensity and duration may explain these different findings. Previous work also demonstrated two distinct pathways involved in light-induced retinal degeneration (40). Bright light-induced apoptosis does not depend on transducin and is accompanied by induction of Ap-1, whereas low light-induced apoptosis is transducin-dependent. Studies by the Chahory and Donovan groups that did not observe Casp3 activation, involved a relatively low doses of light (2 days exposure to 1,000 lux white light or 2 h exposure to 5,000 lux white light, respectively). But those who observed Casp3 activation applied higher intensity and

duration of light exposure (12-24 h exposure to 2,700 lux white light by the Tomita group; 24 h exposure to 3,400 lux white light by the Perche group). We also tested Casp2 expression under higher light intensity exposure. immunoblotting data demonstrated that Casp2 was only up-regulated with 5,000 and 10,000 lux light intensity exposure (Fig. S7, Table S7). So we used 30 min exposure to 10,000 lux white light, a high dose that probably accounts for the observed caspase activation.

Although high level expression of the miR-183/96/182 cluster in retina was identified several years ago, the *in vivo* function and downstream targets of these miRs remain obscure. Adcy6 was confirmed to be one target of the miR-183/96/182 cluster by Xu *et al.* (6) who suggested that this cluster may be involved in circadian rhythm. SLC1A1, a voltage-dependent glutamate transporter, was validated as another target by Krol *et al.* (13), who suggested this cluster functions in glutamate scavenging. Our research now indicates an important role of the miR-183/96/182 cluster in preventing bright light-induced retinal degeneration *in vivo,* and defines Casp2 as a new target that mediates this effect. In fact, phylogenic studies of the 3'-UTR of Casp2 in different mammals defined highly conserved seed regions for miR-183/96/182 (Fig. S1B). A previous *in vivo* study of miR-182 knockout mice showed no phenotypic changes, perhaps because of the functional redundancy of the cluster miR components. Indeed, we found that miR-96 and miR-183 but not miR-182 were up-regulated after bright light exposure suggesting that miR-96 and miR-183 are the cluster components primarily involved in retinal protection. Additional phylogenetic support for this interpretation is that miR-96 and miR-183, but not miR-182 are present in amphioxus (41). MiRs -183, -96 and -182 are suggested to be transcribed in the same pri-miR and all of them were up-regulated in light-adapted retinas (13). But their different expression levels and responses after bright light exposure suggest that their expression, subsequent processing and/or stability are regulated in different ways.

Another intriguing finding of our study was the regional selectivity of light-induced retinal degeneration. The superior retina was far more

10

damaged than the inferior retina. However, we could not detect expression difference of the miR-183/96/182 cluster between superior and inferior retina in any conditions. The same regional difference of vulnerability to intense light was noted previously. In genetically altered mice with defects in the visual cycle, such as *Abca4*^{-/-} *Rdh8*^{-/-} and *Rdh8*^{-/-}*Rdh12*^{-/-} double knockouts (42,43) and an arrestin single knockout (44), retinal degeneration was localized to the inferior region. But in BALB/cJ mice (45) and albino rats (46), retinal damage was more severe in the superior retina than the inferior retina. Differential gene expression in mouse superior and inferior retina has previously been examined by microarray analysis (47), with 27 genes showing an expression difference > 1.5 fold. Among those genes, miR-183/96/182 cluster target sites were predicted in just two, the Efnb2 and Gprc5b 3'-UTRs. Efnb2 is a member of the ephrin family of proteins implicated in development, especially in the nervous system and in erythropoiesis. Gprc5b is a G-protein coupled receptor with an unknown specific function (48). However, the latter protein was suggested to mediate the cellular effects of retinoic acid on the G-protein signal transduction cascade. How these genes are regulated by the miR-183/96/182 cluster and what their roles are in retinal degeneration require future study.

Table1. Predicted miR183 cluster downstream gene candidates.[1]

Name	mRNA	miR	Expression level in retina	Function
Arrdc3	NM_001042591	miR-96, miR-182	12.8	Nervous System Development
Neurod4	NM_007501	miR-96	30.71	
Hes1	NM_008235	miR-96, miR-182	11.3	
Dcx	NM_001110222	miR-96, miR-182, miR-183	0.35	
Ncald	NM_001170866	miR-96, miR-182	29.3	Phototransduction & Visual Cycle
Rarg	NM_001042727	miR-182	2.48	
Gnai3	NM_010306	miR-96, miR-182	9	
Clock	NM_007715	miR-96, miR-182	15.62	Circadian Rhythm
Bhlhe22	NM_021560	miR-182	11.28	
Casp2	NM_007610	miR-96, miR-182	7.17	Apoptosis
Bcl2	NM_009741	miR-96, miR-182	3.41	

[1]List of putative conserved miR-183/96/182 targets in retina. The first column represents the official symbol of the candidate target; the second column is the accession number; the third column indicates which members of the miR-183/96/182 cluster are predicted to target each mRNA; the fourth column shows the mRNA level of the candidate target in retina as measured by deep sequencing; and the fifth column indicates the known function of the candidate target.

REFERENCES

1. Bartel, D. P. (2009) *Cell* **136**, 215-233
2. Bartel, D. P. (2004) *Cell* **116**, 281-297
3. Tanzer, A., and Stadler, P. F. (2004) *J Mol Biol* **339**, 327-335
4. Friedman, R. C., Farh, K. K., Burge, C. B., and Bartel, D. P. (2009) *Genome Res* **19**, 92-105
5. Lagos-Quintana, M., Rauhut, R., Yalcin, A., Meyer, J., Lendeckel, W., and Tuschl, T. (2002) *Curr Biol* **12**, 735-739
6. Xu, S., Witmer, P. D., Lumayag, S., Kovacs, B., and Valle, D. (2007) *J Biol Chem* **282**, 25053-25066
7. Rodieck, R. W. (1998) *The first steps in seeing*, Sinauer Associates, Sunderland, Mass.
8. Arora, A., McKay, G. J., and Simpson, D. A. (2007) *Invest Ophthalmol Vis Sci* **48**, 3962-3967
9. Karali, M., Peluso, I., Marigo, V., and Banfi, S. (2007) *Invest Ophthalmol Vis Sci* **48**, 509-515
10. Damiani, D., Alexander, J. J., O'Rourke, J. R., McManus, M., Jadhav, A. P., Cepko, C. L., Hauswirth, W. W., Harfe, B. D., and Strettoi, E. (2008) *J Neurosci* **28**, 4878-4887
11. Georgi, S. A., and Reh, T. A. (2010) *J Neurosci* **30**, 4048-4061
12. Loscher, C. J., Hokamp, K., Kenna, P. F., Ivens, A. C., Humphries, P., Palfi, A., and Farrar, G. J. (2007) *Genome Biol* **8**, R248
13. Krol, J., Busskamp, V., Markiewicz, I., Stadler, M. B., Ribi, S., Richter, J., Duebel, J., Bicker, S., Fehling, H. J., Schubeler, D., Oertner, T. G., Schratt, G., Bibel, M., Roska, B., and Filipowicz, W. (2010) *Cell* **141**, 618-631
14. Jin, Z. B., Hirokawa, G., Gui, L., Takahashi, R., Osakada, F., Hiura, Y., Takahashi, M., Yasuhara, O., and Iwai, N. (2009) *Mol Vis* **15**, 523-533
15. Mencia, A., Modamio-Hoybjor, S., Redshaw, N., Morin, M., Mayo-Merino, F., Olavarrieta, L., Aguirre, L. A., del Castillo, I., Steel, K. P., Dalmay, T., Moreno, F., and Moreno-Pelayo, M. A. (2009) *Nat Genet* **41**, 609-613
16. Jomary, C., Cullen, J., and Jones, S. E. (2006) *Invest Ophthalmol Vis Sci* **47**, 1620-1629
17. Katai, N., Kikuchi, T., Shibuki, H., Kuroiwa, S., Arai, J., Kurokawa, T., and Yoshimura, N. (1999) *Invest Ophthalmol Vis Sci* **40**, 1802-1807
18. Jomary, C., Neal, M. J., and Jones, S. E. (2001) *Mol Cell Neurosci* **18**, 335-346
19. http://www.sph.uth.tmc.edu/RetNet/.
20. Hahn, P., Lindsten, T., Lyubarsky, A., Ying, G. S., Pugh, E. N., Jr., Thompson, C. B., and Dunaief, J. L. (2004) *Cell Death Differ* **11**, 1192-1197
21. Yoshizawa, K., Kiuchi, K., Nambu, H., Yang, J., Senzaki, H., Kiyozuka, Y., Shikata, N., and Tsubura, A. (2002) *Graefes Arch Clin Exp Ophthalmol* **240**, 214-219
22. Bode, C., and Wolfrum, U. (2003) *Mol Vis* **9**, 144-150
23. Liu, C., Li, Y., Peng, M., Laties, A. M., and Wen, R. (1999) *J Neurosci* **19**, 4778-4785
24. Kumar, S. (2009) *Nat Rev Cancer* **9**, 897-903
25. Ebert, M. S., Neilson, J. R., and Sharp, P. A. (2007) *Nat Methods* **4**, 721-726
26. Maroney, P. A., Chamnongpol, S., Souret, F., and Nilsen, T. W. (2008) *Nat Protoc* **3**, 279-287
27. Soucy, E., Wang, Y., Nirenberg, S., Nathans, J., and Meister, M. (1998) *Neuron* **21**, 481-493
28. Jaissle, G. B., May, C. A., Reinhard, J., Kohler, K., Fauser, S., Lutjen-Drecoll, E., Zrenner, E., and Seeliger, M. W. (2001) *Invest Ophthalmol Vis Sci* **42**, 506-513

13

29. Pittler, S. J., and Baehr, W. (1991) *Proc Natl Acad Sci U S A* **88**, 8322-8326
30. Sakami, S., Maeda, T., Bereta, G., Okano, K., Golczak, M., Sumaroka, A., Roman, A. J., Cideciyan, A. V., Jacobson, S. G., and Palczewski, K. (2011) *J Biol Chem* **286**, 10551-10567
31. Ebert, M. S., and Sharp, P. A. *RNA* **16**, 2043-2050
32. Mustafi, D., Kevany, B. M., Genoud, C., Okano, K., Cideciyan, A. V., Sumaroka, A., Roman, A. J., Jacobson, S. G., Engel, A., Adams, M. D., and Palczewski, K. (2011) *FASEB J*
33. Nabhan, J. F., Pan, H., and Lu, Q. *EMBO Rep* **11**, 605-611
34. Ohsawa, R., and Kageyama, R. (2008) *Brain research* **1192**, 90-98
35. Tosini, G., Pozdeyev, N., Sakamoto, K., and Iuvone, P. M. (2008) *Bioessays* **30**, 624-633
36. Tomita, H., Kotake, Y., and Anderson, R. E. (2005) *Invest Ophthalmol Vis Sci* **46**, 427-434
37. Perche, O., Doly, M., and Ranchon-Cole, I. (2007) *Invest Ophthalmol Vis Sci* **48**, 2753-2759
38. Chahory, S., Keller, N., Martin, E., Omri, B., Crisanti, P., and Torriglia, A. (2010) *Neurochem Int* **57**, 278-287
39. Donovan, M., Carmody, R. J., and Cotter, T. G. (2001) *J Biol Chem* **276**, 23000-23008
40. Hao, W., Wenzel, A., Obin, M. S., Chen, C. K., Brill, E., Krasnoperova, N. V., Eversole-Cire, P., Kleyner, Y., Taylor, A., Simon, M. I., Grimm, C., Reme, C. E., and Lem, J. (2002) *Nat Genet* **32**, 254-260
41. Luo, Y., and Zhang, S. (2009) *Gene* **428**, 41-46
42. Maeda, A., Maeda, T., Golczak, M., and Palczewski, K. (2008) *J Biol Chem* **283**, 26684-26693
43. Maeda, A., Maeda, T., Sun, W., Zhang, H., Baehr, W., and Palczewski, K. (2007) *Proc Natl Acad Sci U S A* **104**, 19565-19570
44. Chen, J., Simon, M. I., Matthes, M. T., Yasumura, D., and LaVail, M. M. (1999) *Invest Ophthalmol Vis Sci* **40**, 2978-2982
45. Zhang, C., Lei, B., Lam, T. T., Yang, F., Sinha, D., and Tso, M. O. (2004) *Invest Ophthalmol Vis Sci* **45**, 2753-2759
46. Tanito, M., Kaidzu, S., Ohira, A., and Anderson, R. E. (2008) *Exp Eye Res* **87**, 292-295
47. Zhu, Y., Natoli, R., Valter, K., and Stone, J. (2010) *Mol Vis* **16**, 740-755
48. Robbins, M. J., Michalovich, D., Hill, J., Calver, A. R., Medhurst, A. D., Gloger, I., Sims, M., Middlemiss, D. N., and Pangalos, M. N. (2000) *Genomics* **67**, 8-18

FIGURE LEGENDS

Figure 1. *MiR-183/96/182 clusters are specifically expressed in photoreceptor cells.* **(A)** Quantification of selected miRs by splinted ligation in 4-month-old wild-type *(wt)*, *Cone-DTA$^{+/-}$* and *Opsin$^{-/-}$* mouse retinas. RNAase-free water was used for a negative control and Let-7 as an internal control. MiR-183, miR-96 and miR-182 were all significantly decreased in *Opsin$^{-/-}$* mice, but unchanged in *Cone-DTA$^{+/-}$* mice. Compared to *wt*, MiR-107 was unchanged in *Cone-DTA$^{+/-}$* and *Rho$^{-/-}$* mice. **(B)** Quantification of selected miRs by splinted ligation in the retina of 4-month-old *wt* mice, *rd1/rd1* mutant mice (29) and P23H opsin knock-in homozygous mice (P23H)(30). Hela cells, derived from a human cervical cancer cell line were used as a negative control because these cells do not express the miR-183/96/182 cluster. Compared to *wt* retina, miR-183, miR-96 and miR-182 were decreased in rd1/rd1 and P23H mutant retina but Let-7 stayed the same as in *wt* retina and miR-125a even increased slightly in mutant mice.

Figure 2. Creation of miR-183/96/182 cluster sponge transgenic mice. **(A)** PCR genotyping of the miR-183/96/182 cluster sponge in transgenic mice: **a.** Three transgenic lines are shown with different levels of transgene detected by PCR. Rd_For/Pde_Rev and Pde_For/Pde_Rev primers were used to confirm the absence of the *Pde6b^{rd1}* mutant allele. PCR of β actin was used as a control for genomic DNA preparations. **b.** Shown are absolute transgene copy numbers in heterozygotes calculated by real time PCR in different mouse lines. These were 2.1± 0.4 in #1135, 1.3± 0.1 in #1128 and 7.0±1.0

15

almost identical in the inferior retina of untreated and light-exposed mice, but were reduced from about 50 μm to 20 μm in the superior retina of transgenic mice after bright light exposure. Abbreviations: INL, inner nuclear layer; ONL, outer nuclear layer; ONH, optic nerve head. Error bars represent standard errors of the means (n=4). **(C)** Expression levels of the miR-183/96/182 cluster were the same in mouse superior and inferior retina: LNA-based real time PCR showed that miR-96 and miR-183 but not miR-182 increased after light exposure in both *wt* and transgenic mice. None of these three miRs were differentially expressed in the superior and inferior retina under these conditions. Error bars represent standard errors of the means (n=3).

Figure 5. *Identification of candidate targets of miR-183/96/182 cluster miRs.* Predicted miR-183/96/182 targets are listed in **Table 1** where their NCBI reference sequences, putative binding miRs, expression levels in retina and known functions are also shown. **(A)** Comparison of candidate target mRNA levels between 4-month-old *wt* and transgenic mice by real-time PCR. Four genes, namely Arrdc3, Neurod4, Clock and Casp2, out of 11 candidates showed significant increases in transgenic mice. **(B)** Confirmation of these target genes by real-time PCR. mRNA levels were compared between transgenic mice and their *wt* littermates. Arrdc3, Neurod4, Clock, and Casp2 mRNAs were all up-regulated in retinas from all three transgenic mouse lines. Real-time PCR results were all normalized to GAPDH. Error bars represent standard errors of the means (n=3), * *p*<0.01. **(C)** Target gene changes in stable cell lines. **a.** mRNA levels of indicated genes in three stable cell lines were detected by real time PCR; GAPDH was used as an internal control. mRNA levels of Arrdc3 in miR-96 stable cells were 62% of those in NIH3T3 cells, but were essentially unchanged in miR-182 stable cells and even increased 1.3- fold in miR-183 stable cells. Clock's mRNA level remained the same in all cell lines. mRNA levels of Casp2 in miR-96 and miR-182 stable cells were 42% and 57% of those in NIH3T3 cells but were unchanged in miR-183 stable cells. Error bars represent the standard errors of the means (n=3), * *p*<0.01. **b.** Protein levels of both pro- and cleaved-Casp2 in three stable cell lines were documented by immunoblotting with an anti-Casp2 antibody. Both pro-Casp2 and cleaved-Casp2 were decreased in miR-96 and miR-182 stable cells but not in miR-183 stable cells. β-Tubulin was used as the internal control. **(D)** Confirmation of miR-183/96/182 cluster targets by luciferase assay. miR-96 repressed luciferase activity by 47% in Arrdc3, 57% in Neurod4 and 57% in Casp2 compared with the parental pGL3P vector; miR-182 repressed luciferase activity by 41% in Arrdc3 and 39% in Casp2 compared with the empty vector; and miR-183 made no difference in all target genes. As a negative control, luciferase activity of the empty pGL3P vector was not affected by any miR-183/96/182 cluster miRs. All data were normalized to those obtained with the pGL3P vector alone. Error bars represent standard errors of the means (n=3), * *p*<0.01.

Figure 6. *MiR-183/96/182 cluster miRs repress Casp2 during light exposure.* **(A)** Both miR-183/96/182 cluster miRs and Casp2 expression levels increased in 4-month-old wild type mice after 10,000 Lux white bright light exposure. **a.** Real time PCR shows Casp2 was modestly up-regulated 12 to 24 h after light exposure. **b.** Splinted ligation data show that miR-96 and miR-183 but not miR-182 increased 12 to 24 h after light exposure. **(B)** Repression of Casp2 is not observed in sponge transgenic mice. **a.** Casp2 mRNA levels increased more after light exposure in transgenic mice than in *wt* mice as demonstrated by real-time PCR. **b.** Immunoblotting analysis confirms the greater increase of Casp2 protein levels and the enhanced cleavage of bid protein in light-exposed transgenic mice. **(C)** Immunohistochemistry of retinas stained with peanut agglutinin lectin (PNA) for cones and anti-opsin (1D4) antibody for rods; DAPI was used as a counterstain to detect cell nuclei. DMSO-treated 4-month-old sponge transgenic mice showed severe retinal degeneration after light-exposure whereas Z-VDVAD-FMK-treated 4-month-old sponge transgenic mice showed only moderate retinal damage. *Wt* mouse retinas appeared normal in both conditions. Scale bars: 10 μm. **(D)** Thicknesses of the outer nuclear retinal layer measured 2 weeks after light exposure are shown. Injection of Z-VDVAD-FMK had a partial protective effect

16

against light-induced structural damage to the retina of transgenic mice. As in transgenic mice, ONL thicknesses in retinas of Z-VDVAD-FMK-treated transgenic mice were about 30 μm in the superior area, whereas in the same area, ONL thicknesses of DMSO-treated transgenic mice were only about 20 μm. Retinas from *wt* mice were normal, with ONL thicknesses of about 50 μm. Error bars represent standard errors of the means (n=4). Abbreviations: GCL, ganglion cell layer; IPL, inner plexiform layer; INL, inner nuclear layer; OPL, outer plexiform layer; ONL, outer nuclear layer; ELM, external limiting membrane; IS, inner segment; OS, outer segment; RPE, retinal pigmented epithelium; ONH, optic nerve head. **(E) a.** Immunoblotting data show that without Z-VDVAD-FMK treatment, the opsin level in four-month-old sponge transgenic mouse retina was only 40% of that in *wt* littermate retina after light exposure and the mw-opsin level in the transgenic mouse retina was only 70% of that in *wt retina.* But with Z-VDVAD-FMK treatment, the opsin level in four-month-old sponge transgenic mouse retina was 50% that in the retina of *wt* littermates after light exposure and the mw-opsin level in transgenic retina was even slightly increased. Statistical analyses are shown in **b**, Error bars represent standard errors of the means (n=3), * $p<0.05$.

Figure 7. *Model of miR-183/96/182 cluster-mediated regulation of Casp2 protein and function in retinal degeneration.* miR-183/96/182 cluster miRs repress Casp2 expression after bright light exposure, thereby protecting photoreceptors from apoptosis.
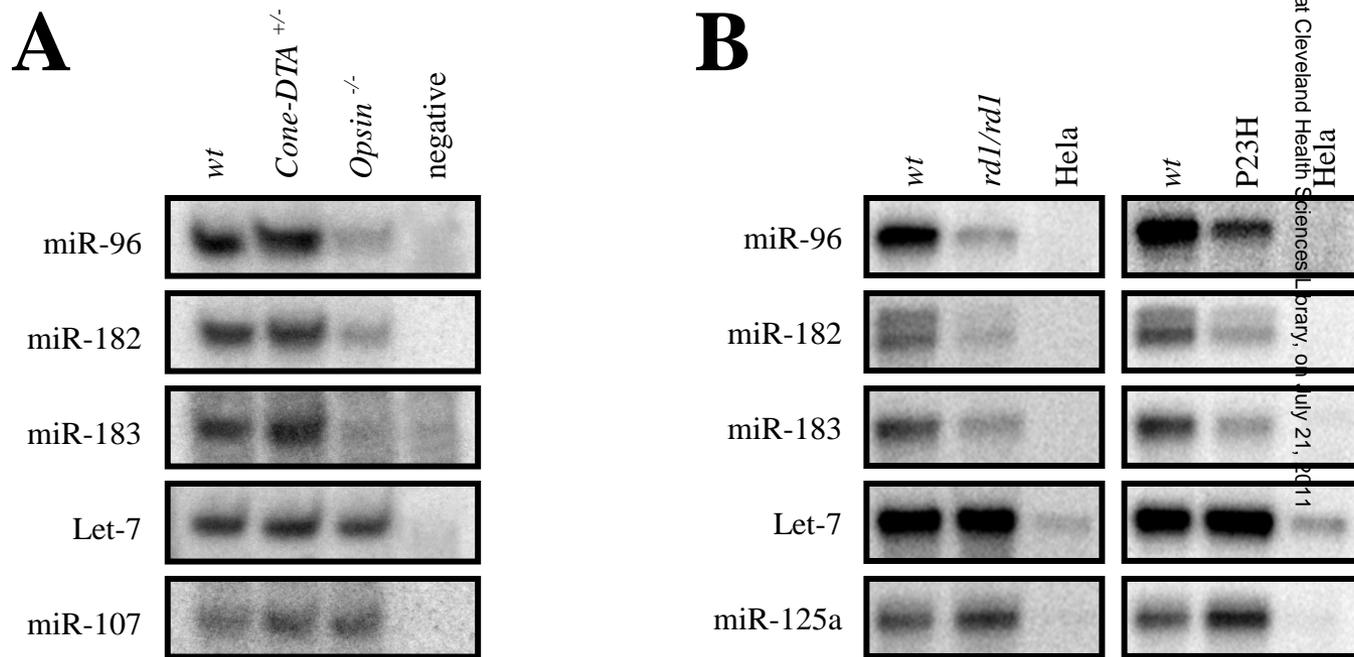
A

	wt	*Cone-DTA* [+/-]	*Opsin* [-/-]	negative
miR-96				
miR-182				
miR-183				
Let-7				
miR-107				

B

	wt	*rd1/rd1*	Hela	*wt*	P23H	Hela
miR-96						
miR-182						
miR-183						
Let-7						
miR-125a						
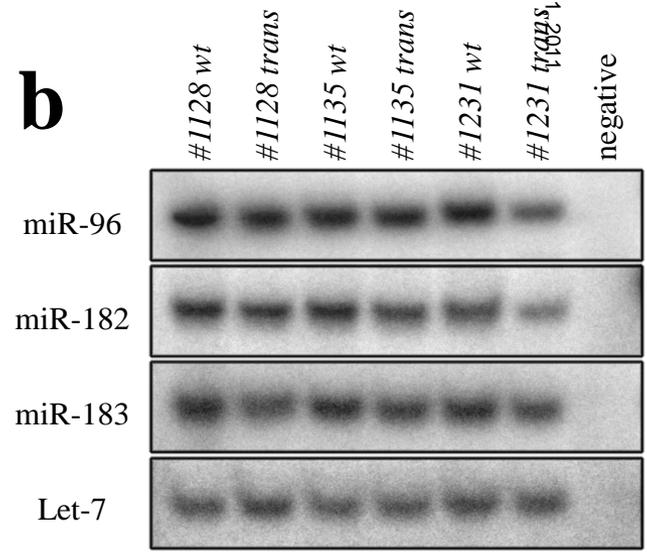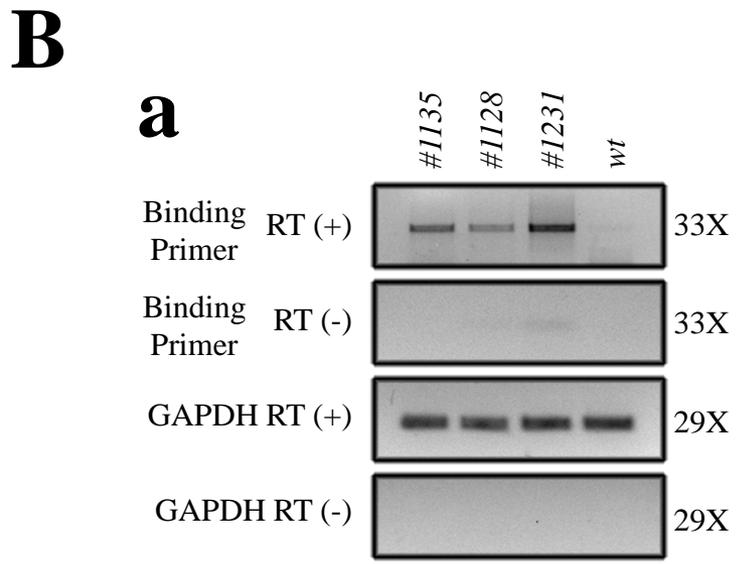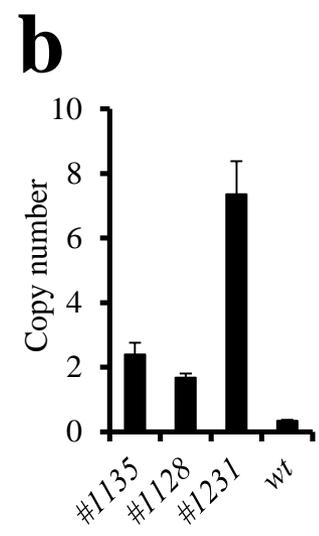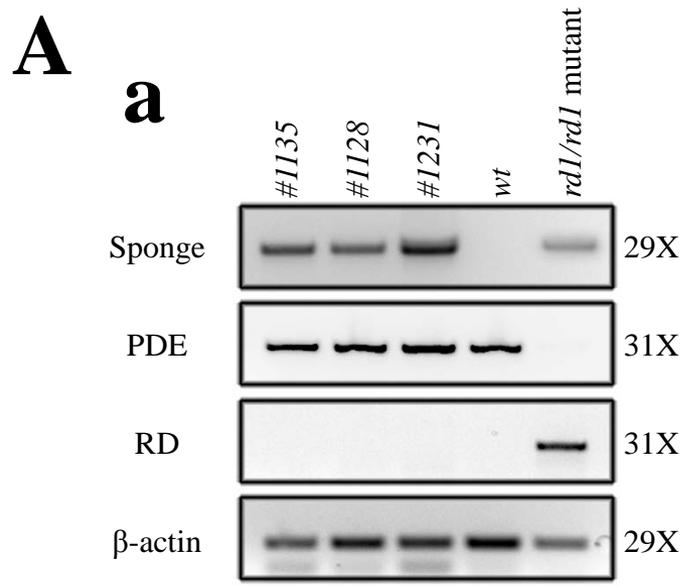
Figure 1

Figure 2

Figure 3

C

a

Figure 3

b

	wt			transgene		
	0 min	10 min	30 min	0 min	10 min	30 min

rod opsin

mw-opsin

β-tubulin

A

B

Figure 4

C

miR-96

miR-182

miR-183

Figure 4

A

Normalized expression

■ *wt*
□ transgene

Arrdc3, Neur..., Clock, Casp2, Bhlh..., Ncald, Gnai, Rarg, Bcl2, Hes1, Tbl1, Dcx

B

Normalized expression

■ *#1128 wt*
□ *#1128 trans*
■ *#1135 wt*
□ *#1135 trans*
■ *#1231 wt*
□ *#1231 trans*

Arrdc3, Neuro4, Clock, Casp2

C

a

Normalized expression

■ NIH3T3   ■ miR-96
■ miR-182 □ miR-183

Arrdc3, Clock, Casp2

b

NIH3T3, miR-96, miR-182, miR-183

49 kDa pro-Casp2 →

12 kDa cleaved-Casp2 →

β-tubulin →

Figure 5

D

Figure 5

A

a

Casp2 level

b

0 h 1 h 3 h 6 h 12 h 24 h 72 h

miR-96

miR-182

miR-183

Let-7

B

a

Casp2 level

not treated | light exposed
wt
not treated | light exposed
transgene

b

wt   transgene

not treated
Light exposed
not treated
Light exposed

49 kDa
pro-Casp2

12 kDa
cleaved-Casp2

Bid

tBid

β-tubulin

Figure 6

C

D

E

a

<u>*wt*</u>   <u>transgene</u>

Z-VDVAD   DMSO   Z-VDVAD   DMSO

opsin

mw-opsin

β-tubulin

b

opsin

Z-VDVAD	DMSO	Z-VDVAD	DMSO

mw-opsin

Z-VDVAD	DMSO	Z-VDVAD	DMSO

Apoptosis

Light

Caspase-2

miR-96
miR-182
miR-183

Figure 7